HHS Public Access

Author manuscript

Cell Rep. Author manuscript; available in PMC 2022 May 29.

Published in final edited form as:

Cell Rep. 2022 April 05; 39(1): 110633. doi:10.1016/j.celrep.2022.110633.

Diurnal rhythms in cholinergic modulation of rapid dopamine signals and associative learning in the striatum

Taylor A. Stowe[1], **Elizabeth G. Pitts**[1], **Amy C. Leach**[1], **Melody C. Iacino**[1], **Farr Niere**[1], **Benjamin Graul**[2], **Kimberly F. Raab-Graham**[1], **Jordan T. Yorgason**[2], **Mark J. Ferris**[1,3,*]

[1]Department of Physiology and Pharmacology, Wake Forest School of Medicine, 1 Medical Center Blvd., Winston-Salem, NC 27157, USA

[2]Department of Cellular Biology and Physiology, Neuroscience Center, Brigham Young University, Provo, UT 84602, USA

[3]Lead contact

SUMMARY

Dysregulation of biological rhythms plays a role in a wide range of psychiatric disorders. We report mechanistic insights into the rhythms of rapid dopamine signals and cholinergic interneurons (CINs) working in concert in the rodent striatum. These rhythms mediate diurnal variation in conditioned responses to reward-associated cues. We report that the dopamine signal-to-noise ratio varies according to the time of day and that phasic signals are magnified during the middle of the dark cycle in rats. We show that CINs provide the mechanism for diurnal variation in rapid dopamine signals by serving as a gain of function to the dopamine signal-to-noise ratio that adjusts across time of day. We also show that conditioned responses to reward-associated cues exhibit diurnal rhythms, with cue-directed behaviors observed exclusively midway through the dark cycle. We conclude that the rapid dopamine signaling rhythm is mediated by a diurnal rhythm in CIN activity, which influences learning and motivated behaviors across the time of day.

Graphical abstract

*Correspondence: mferris@wakehealth.edu.

AUTHOR CONTRIBUTIONS

Conceptualization, T.A.S. and M.J.F.; formal analysis, T.A.S. and F.N.; investigation, T.A.S., A.C.L., M.C.I., F.N., B.G., and J.T.Y.; resources, M.J.F. and K.F.R.-G.; writing — original draft, T.A.S., E.G.P., and M.J.F.; writing — review & editing, T.A.S., E.G.P., A.C.L., M.C.I., F.N., B.G., K.F.R.-G., J.T.Y., and M.J.F.; funding acquisition, M.J.F.

SUPPLEMENTAL INFORMATION

Supplemental information can be found online at https://doi.org/10.1016/j.celrep.2022.110633.

DECLARATION OF INTERESTS

The authors declare no competing interests.

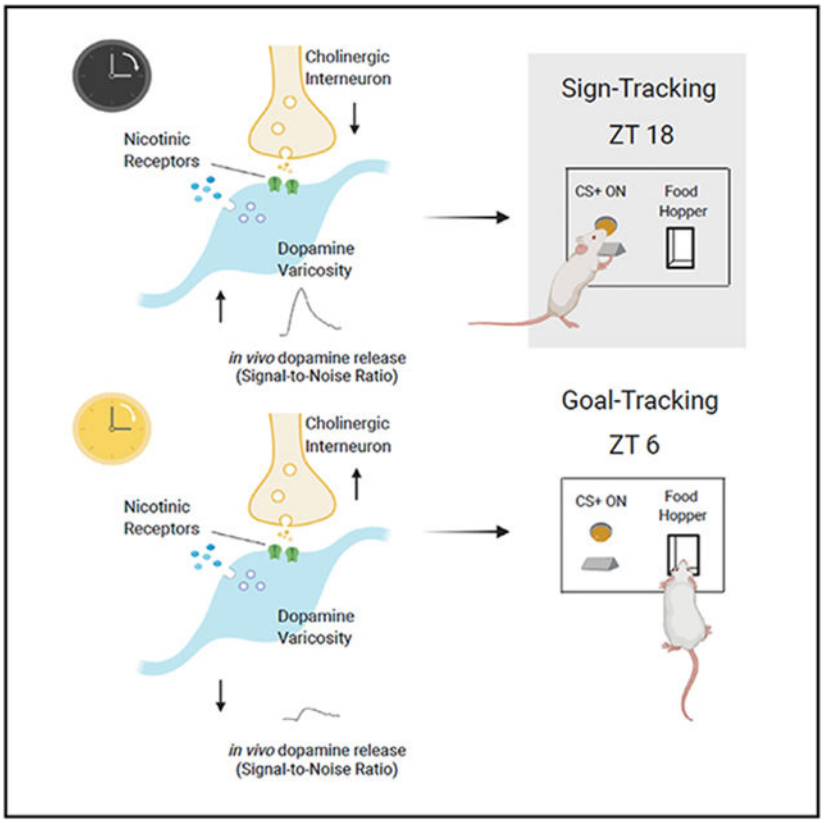

In brief

Dopamine signals in the striatum are critical for learning and motivation. Stowe et al. show that diurnal rhythms in rapid dopamine signaling in the striatum are mediated by time-of-day shifts in cholinergic interneuron control of dopamine. These systems work together to mediate time-of-day changes in learning and motivated behaviors.

INTRODUCTION

Biological rhythms are essential for survival and can be entrained to diurnal (i.e., light/dark) cycles. This includes diurnal variations in behaviors and physiological systems in the central nervous system (Parekh et al., 2015). For example, there are diurnal patterns in the function of the mesolimbic dopamine (DA) system, such as higher extracellular DA levels and DA metabolites in the *nucleus accumbens* (NAc) core during the dark/active cycle of rodents (Paulson and Robinson, 1994; Castañeda et al., 2004; Dibner et al., 2010; Ferris et al., 2014). However, prior research has largely ignored the mechanisms of real-time, subsecond DA rhythms in the NAc. This is a major gap in our understanding because rapid DA signaling (as opposed to extracellular DA tone) is a neural substrate for learning, motivation, and goal/reward seeking (Robinson et al., 2002; Cheer et al., 2004; Adamantidis et al., 2007; Saunders et al., 2014). Clinical and preclinical data have shown that reward-associated behaviors vary across time of day (Negus et al., 1995; Roberts et al., 2002; Ren et al., 2009). A more complete understanding of the temporal architecture of rapid DA signals

and mechanisms that influence DA rhythms is necessary for insight into how and why they are dysregulated in disease states. Specifically, determining mechanisms for time-of-day variation in DA release magnitude in the NAc core will be imperative for understanding the etiology of, and therapeutic approaches for, disorders that are rooted in perturbations of learning and motivation.

Here we used fast-scan cyclic voltammetry (FSCV) combined with electrical and optogenetic stimulation of DA terminals and cholinergic interneurons (CINs) as well as electrophysiology to examine time-of-day variation in DA and local regulators of DA release magnitude in the NAc. We also used a Pavlovian conditioned approach (PCA) to determine diurnal variations in conditioned responses to reward-associated cues that are mediated by DA in the NAc. Exploring the dynamic rhythms of the neural substrates for motivation and learning in a healthy brain, as opposed to a single time of day, will form a more coherent understanding of basic principles of brain function (Whitton et al., 2018). It will also provide a rationale for targeting neurochemical and receptor systems that are mechanistically linked to daily oscillations in learning and motivation to restore normal function in individuals with neuropsychiatric disorders.

RESULTS AND DISCUSSION

Diurnal variation of DA release in the NAc core

Mesolimbic and nigrostriatal DA systems have been shown to exhibit circadian and diurnal rhythms. For example, DA transporter (DAT) function, extracellular DA tone, and DA metabolite levels vary across time of day (Webb, 2017; Ferris et al., 2014). Exocytotic DA release magnitude ($[DA]_o$) after electrical stimulation in rodent brain slices peaks around mid-light (zeitgeber time [ZT] 6) and is lowest mid-dark (ZT 18) (Ferris et al., 2014). We sought to discover the mechanism for time-of-day variation in $[DA]_o$. This is critical for our understanding of signals that mediate motivation, learning, reinforcement, and goal-directed behaviors (Robinson et al., 2002; Cheer et al., 2004; Adamantidis et al., 2007; Saunders et al., 2014). We utilized FSCV to examine $[DA]_o$ in the NAc core (Figure 1A) across four time points that span a 12:12 h light:dark cycle in rats (Figure 1B). We first found diurnal rhythms in $[DA]_o$ in response to single-pulse electrical stimulation at ZT 1 (1 h into light), ZT 6, ZT 13 (1 h into dark), and ZT 18 (Figures 1B and 1C). $[DA]_o$ exhibits an inverted U-shaped curve across time of day, with significantly higher release at ZT 6 (mid-light) and ZT 13 (early dark) in comparison with ZT 1 and ZT 18 (main effect of time: $F_{(3,16)} = 11.46$, $p = 0.0003$).

We also examined short-term plasticity of release (i.e., facilitation or depression of $[DA]_o$) using paired-pulse ratios (PPRs) (Figure S1A; Condon et al., 2019; Cragg, 2003). There was significant diurnal variation in PPRs at shorter inter-stimulus intervals (ISIs) (0.1–0.8 s) but not at ISIs longer than 1 s across all ZT points. Paired-pulse facilitation of $[DA]_o$ was observed at ZT 1 and ZT 13, and paired-pulse depression was observed at ZT 6 (ZT × ISI interaction: $F_{(3,158)} = 4.331$, $p < 0.0001$) (Figure S1A). We also found diurnal rhythms in DA release across multiple stimulation amplitudes (Figure S1B; ZT × amplitude interaction: $F_{(3,27)} = 4.973$, $p < 0.001$). Last, we repeated FSCV in a cohort of female rats and found similar $[DA]_o$ patterns as in male rats, with higher $[DA]_o$ at ZT 6 in comparison with ZT

18 (Figure S2A; $t_{(9)}$=2.651, p = 0.0264). These data collectively support the presence of diurnal rhythms in DA dynamics across a range of stimulation parameters, such as number of stimulations and amplitude. We next determined whether diurnal rhythms persisted in $[DA]_o$ across a range of stimulation patterns that specifically model *in vivo* firing patterns of DA neurons.

Diurnal variation of DA release magnitude across a range of physiologically relevant stimulation frequencies

Ventral tegmental area (VTA) DA neurons exhibit firing patterns of varying frequencies that correspond to specific behaviors or motivational states. Research has determined at least two modes of firing based on frequency: tonic and phasic firing (Grace and Bunney, 1984). DA neurons are thought to mediate effort allocation during tonic firing, which is a lower-frequency mode (~5 Hz) (Saunders and Collins, 2020). In contrast, phasic firing (≥20 Hz) is associated with learning and motivation and occurs in response to salient environmental stimuli (Steinberg et al., 2013; Sharpe et al., 2017).

Thus, we used single- and multiple-pulse (5 pulses [p]) stimulations across a range of frequencies (5, 10, 20, and 100 Hz) to model the full range of DA neuron firing at the four time points assessed previously. There was a main effect of frequency ($F_{(4, 75)}$ = 5.865, p = 0.0004) with generally higher magnitude $[DA]_o$ as the frequency increased for ZT 1, ZT 13, and ZT 18 (Figure 1D). ZT 6 exhibited an inverted U-shaped curve as the frequency increased, with peak $[DA]_o$ at 20-Hz stimulation. $[DA]_o$ exhibited a diurnal pattern of release similar to that of a single pulse, with release significantly lower at ZT 1 compared with all other time points, and ZT 6 had significantly higher DA release than ZT 18 (main effect of time point: $F_{(3, 75)}$ = 22.26 p < 0.0001) (Figure 1D).

We next examined the relationship between stimulations that mimic tonic-like firing and phasic-like firing with ratios of 20-Hz stimulation over single-pulse stimulation (Zhang et al., 2009). Phasic/tonic ratios were significantly higher at ZT 18 (mid-dark) than at all other time points (Figure 1E) (main effect of time: $F_{(3,19)}$ = 11.13, p = 0.003). Similar to male rats, female rats also showed higher phasic/tonic ratios at ZT 18 in comparison with ZT 6 (Figure S2B; $t_{(6)}$ = 2.542, p = 0.044). These results demonstrate that DA phasic/tonic signals may be elevated at times of day when DA-dependent behaviors, such as learning and motivation, are most necessary for survival and that these patterns are similar in males and females. However, this time of day may reflect when an individual may have heightened vulnerability to maladaptive behaviors, like taking drugs. We next aimed to expand on this by determining the mechanism governing these variations in DA dynamics and whether variations in learning and motivated behavior map onto these rhythms.

Diurnal variation in the effects of nicotinic acetylcholine receptor modulation of DA release

Homosynaptic and heterosynaptic modulators play a key role in mediating $[DA]_o$ at terminals (Nolan et al., 2020). Thus, we sought to delineate which heterosynaptic modulator is potentially driving this diurnal pattern within $[DA]_o$. One strong candidate for a potential mechanism is DA modulation by accumbal CINs (Bennett and Wilson, 1999; Zhou et al., 2001). CINs are strong regulators of $[DA]_o$ magnitude via release of acetylcholine

(ACh) acting on nicotinic acetylcholine receptors (nAChRs) located directly on DA axons/terminals (Rice and Cragg, 2004). For instance, ACh can drive $[DA]_o$ independent of VTA-mediated action potentials (Yorgason et al., 2017; Threlfell et al., 2012; Cachope et al., 2012). Antagonism or desensitization of nAChRs on DA varicosities alters $[DA]_o$ in a frequency-dependent manner (Pidoplichko et al., 1997; Rice and Cragg, 2004; Siciliano et al., 2017). Therefore, we investigated the hypothesis that there is diurnal variation in CIN-induced modulation of $[DA]_o$. We hypothesized that there is greater CIN mediated enhancement of $[DA]_o$ at times of day when $[DA]_o$ is peaking (i.e., ZT 6).

To address the potential role of ACh, we first utilized dihydro-β-erythroidine hydrobromide (DHβE), a β2-selective nAChR antagonist, as a pharmacological tool to determine the effects of nAChR antagonism on $[DA]_o$ resulting from electrical stimulation. We focused on β2-containing nAChRs because these are located on DA terminals, and CINs activate these receptors to increase $[DA]_o$ probability (Zhou et al., 2001; Rice and Cragg, 2004; Brimblecombe et al., 2018). There was a significantly greater decrease in $[DA]_o$ after bath application of DhβE at ZT 6 in comparison with ZT 18 (Figure 1F) ($t_{(9)}$ =2.879, $p < 0.05$), suggesting greater amplification from ACh acting via nAChRs on DA terminals at ZT 6. Thus, it is possible that the magnitude of ACh release from CINs exhibits intrinsic rhythms, which may account for time-of-day rhythms in $[DA]_o$ magnitude.

Diurnal variation of DA release *in vivo*

To further test intrinsic rhythms in CIN activity and CIN control of $[DA]_o$, we next used *in vivo* voltammetry to electrically stimulate the VTA and record $[DA]_o$ from the NAc core (Figure 1G). Electrical stimulation in slice preparation in the NAc core is not selective and allows local modulators, like ACh, to govern $[DA]_o$ (Berke, 2018). Moving the stimulation away from the NAc and to the VTA prevents direct stimulation of CINs. $[DA]_o$ was higher at ZT 18 in comparison with ZT 6 (Figure 1H; $t_{(7)} = 3.463$, $p = 0.0105$) when stimulating the VTA. These data are opposite of what we found when using the same technique to directly stimulate the NAc in brain slice preparations (Figure 1I). The pattern of $[DA]_o$ exhibited after VTA stimulation, in which the number of pulses and frequency mimics phasic firing of VTA DA neurons, corresponds with the pattern of phasic/tonic ratios in our *ex vivo* preparation. These data also correspond with previous research that has found an increase in tyrosine hydroxylase (TH) levels, DA metabolites, and VTA neuron firing during the dark cycle (DePoy et al., 2017; McClung, 2007; Webb, 2017).

Diurnal rhythms in CIN activity

All prior experiments have indirectly measured variation in CIN activity via CIN control of DA. To further test intrinsic rhythms in CIN activity, electrophysiology experiments were performed to determine whether there were diurnal rhythms in CIN activity consistent with patterns in $[DA]_o$. Cell-attached recordings were performed from CINs in the NAc core from animals euthanized at ZT 6 and ZT 18. We found significantly higher tonic firing at ZT 6 (3 ± 0.6 Hz) in comparison with ZT 18 (1.7 ± 0.4 Hz; Figures 1J and 1K; $t_{(24)} = 2.023$, $p < 0.05$), which suggests that the enhanced effects of DhβE on $[DA]_o$ at ZT 6 could in part be due to enhanced CIN excitability.

Diurnal variation in DA release is mediated by CINs

Electrical stimulations used in prior FSCV experiments cause burst firing of CINs and release of ACh, which, in turn, has been shown to robustly amplify $[DA]_o$ magnitude (Rice and Cragg, 2004; John and Jones, 2006; Berke, 2018). We have several lines of indirect evidence showing that our stimulation is causing CINs to amplify $[DA]_o$ to a much greater extent at ZT6 compared with ZT18 (Figure 1K). For more direct evidence, we designed a series of experiments using optogenetic approaches to selectively modulate DA axons and CIN activity. We first used blue light to exclusively activate DA terminals in the NAc core. If variation in $[DA]_o$ is caused by differential contribution of ACh amplification caused by electrical stimulation, then selective activation of DA axons (where CIN stimulation is absent) should disrupt the rhythm observed when applying electrical stimulation (where CIN stimulation is present). Specifically, we should observe greater decreases in $[DA]_o$ magnitude at ZT 6 when comparing blue light with electrical stimulation within the same tissue.

TH-cre rats were bilaterally infused with a virus into the VTA to express the light-activated opsin (channelrhodopsin2 [ChR2]) selectively on NAc terminals. We then used light stimulation combined with FSCV to excite only DA axons in the NAc core (Figure 2A). Figure 2B shows immunohistochemical verification of ChR2 expression in TH-positive cells in the VTA (top row) and NAc (bottom row). Here we focused on the two time points where we saw the greatest difference in $[DA]_o$ and phasic/tonic ratios (ZT 6 and ZT 18) and compared this with electrical stimulation of the NAc $[DA]_o$ from the same brain slices. Light stimulation of DA terminals in the NAc resulted in significantly higher $[DA]_o$ at ZT 18 than ZT 6 (Figures 2C and 2D) ($t_{(8)} = 3.388$, $p < 0.05$), which is opposite of electrically stimulated $[DA]_o$ (Figures 2C and 2E) and similar to VTA stimulation performed *in vivo* (Figure 1H). We also found that applying DHβE did not decrease $[DA]_o$ after light stimulation, which supports the hypothesis that $[DA]_o$ was not modulated by ACh during light stimulation (Figure 2D).

We next used optogenetics to selectively activate CINs to assess the sufficiency of ACh release to produce the diurnal rhythms in $[DA]_o$ observed using electrical stimulation (Figure 3A). We bilaterally infused a virus into the NAc core of choline acteyltransferase (ChAT)-cre rats to selectively express ChR2 on CINs. Figure 3B shows immunohistochemical verification of ChR2 expression in ChAT-positive cells in the NAc. We compared CIN-induced $[DA]_o$ resulting from light stimulation with electrically stimulated $[DA]_o$. Light stimulation of CINs resulted in $[DA]_o$ that was significantly higher at ZT 6 than ZT 18 (Figures 3C and 3D) ($t_{(5)} = 4.730$, $^{**}p < 0.0052$). Electrical stimulation in these brain slices produced the same relationship between ZT 6 and ZT 18 as light stimulation of CINs, with greater $[DA]_o$ at ZT 6 (Figures 3C and 3F) ($t_{(7)} = 3.759$, $^{**}p < 0.0071$). Finally, $[DA]_o$ to light stimulation of CINs was completely abolished after application of DHβE (Figure 3E), which confirms that $[DA]_o$ with light stimulation was from ACh modulation of $[DA]_o$ via nAChRs. These data, together with the CIN firing data, indicate that CIN regulation of $[DA]_o$ expresses a diurnal rhythm with greatest ACh effects at ZT 6.

Diurnal variation in conditioned responses to reward-associated cues

We next utilized a behavioral paradigm that measured conditioned responses to rewards and reward-associated cues to determine whether variations in these conditioned responses coincided with fluctuations in $[DA]_o$. PCA can determine the associative learning of rewards and their associated cues and examine conditioned responses to these cues (Flagel et al., 2007). PCA designates distinct behavioral repertoires, like sign-tracking and goal-tracking behaviors, that are differentially dependent on DA signaling in the NAc (Saunders and Robinson, 2013; Flagel et al., 2011). For example, sign tracking is a form of associative learning where approach behavior is directed toward reward-associated cues and is dependent on DA signaling in the NAc. Goal tracking is approach behavior directed toward the rewards and is not dependent on DA signaling in the NAc (Flagel et al., 2011; Clark et al., 2013). PCA is also useful as a model of drug abuse vulnerability because rats that exhibit heightened sign-tracking behaviors (i.e., cue directed) show increased acquisition rates of cocaine at lower doses (Beckmann et al., 2011). Thus, we first determined diurnal variations in conditioned responses to rewards and reward-associated cues by using the PCA midway through the light cycle (ZT 6) and midway through the dark cycle (ZT 18) (Figures 4A and 4B) in separate groups of rats.

By the third PCA session, rats begin exhibiting goal-tracking (Figure 4C; main effect of session: $F_{(4, 124)} = 2.994$, $p = 0.0213$) and/or sign-tracking behaviors (Figure 4D; main effect of session: $F_{(4, 194)} = 4.724$, $p = 0.0012$), with sign-tracking behaviors primarily expressed during ZT 18. Average head entries (average of last 3 sessions) into the food hopper during the conditioned stimulus presentation (CS+) were not significantly different between time points, which supports that rats were awake and engaged in the task during both times (Figure 4E). In contrast, average CS+ contacts (average of last 3 sessions), were significantly higher at ZT 18 (Figure 4F; $t_{(5)} = 5.460$, $p < 0.0001$). We also found no significant differences between average latency to first head entry (Figure 4G) but did find the average latency to first CS+ contact to be significantly lower at ZT 18 (Figure 4H; $t_{(25)} = 2.400$, $p = 0.0242$). Thus, CS+ contacts (i.e., sign-tracking behaviors) were exclusive to rats at ZT 18. This result agrees with a recent report showing an increase in motivation for food reward in rodents during the dark cycle (Acosta et al., 2020) and with previous reports of increased responses for reinforcing electrical brain self-stimulation in rodents with a peak during the dark period (Terman and Terman, 1970, 1975). These behavioral data also correspond with our data showing higher phasic/tonic ratios at ZT 18.

We next aimed to determine whether diurnal variation in ACh modulation of $[DA]_o$ governs these behavioral responses. We utilized nicotine as a pharmacological tool to determine the presence of diurnal variations in nAChR modulation of sign-tracking behaviors and phasic/tonic ratios.

Nicotine selectively enhances sign tracking and phasic/tonic ratios during the dark cycle

Nicotine has been shown to enhance sign-tracking behaviors (Palmatier et al., 2013). Thus, we determined whether diurnal variations were present for nicotine's effects on sign-tracking behaviors. After 5 PCA sessions in which no nicotine was administered, we ran a test session in which rats received a 0.4 mg/kg subcutaneous nicotine injection 15 min

before a test PCA session. CS+ contacts were significantly enhanced by nicotine exclusively at ZT 18 in comparison with ZT 6 (Figure 4I; $t_{(20)} = 2.597$, $p = 0.0172$) and in comparison with saline injection at ZT 18 in a separate cohort of animals (Figure S3B; $t_{(12)} = 2.452$, $p = 0.0305$). Nicotine had no effect on CS+ contacts at ZT 6 in comparison with saline injection at ZT 6 in a separate cohort of animals (Figure S3A; $t_{(15)} = 6.345$, $p = 0.5353$). In subsequent FSCV studies performed the day after PCA testing in the same animals, nicotine applied to the slice significantly enhanced $[DA]_o$ phasic/tonic ratios at ZT 18 in comparison with ZT 6 (Figure 4J; $t_{(16)} = 3.818$, $p = 0.0015$), which is consistent with the increase in sign-tracking behaviors after nicotine pretreatment. These data support that nAChR modulation of $[DA]_o$ by nicotine is more sensitive, at least acutely, at ZT 18. Our previous experiments showed that ZT 6 rats have higher CIN activity and ACh-mediated facilitation of DA release, which, we hypothesize, masks/blocks the effects nicotine, as a nAChR agonist, would have on performance in the PCA task.

Conclusions

We report several functions of rapid DA signals and CINs working in concert in the striatum. First, we report that the DA signal-to-noise ratio varies greatly across time of day, and phasic signals are magnified during specific times in the circadian cycle when reward seeking (for food, reproduction, etc.) would be advantageous for the organism. Second, we show that CINs provide the mechanism for diurnal variation in $[DA]_o$ and serve as a gain of function to the DA signal-to-noise ratio that adjusts across time of day. Indeed, prior reports (Threlfell et al., 2012; Cachope et al., 2012) established that CINs are well poised to evoke the release of DA and modulate the frequency-dependent nature of $[DA]_o$ (Rice and Cragg, 2004; Zhang and Sulzer, 2004) via nAChRs located on axonal varicosities of DA neurons. We report that diurnal variations exist in conditioned responses to reward-associated cues in a manner consistent with fluctuations in DA phasic/tonic ratios. Last, we also found that nicotine pre-treatments enhanced cue-directed behaviors exclusively at ZT 18.

We previously reported the importance of DAT function/DA uptake in diurnal shifts in extracellular DA tone as well as shifts in D2 autoreceptor (D2AR) function (Ferris et al., 2014). Consistent with the current study, the prior report eliminated DAT and D2AR function as a mechanism for increased $[DA]_o$ magnitude at ZT 6. First, DA uptake was fastest when $[DA]_o$ was highest at ZT 6 and slowest when $[DA]_o$ was low at ZT 18. This relationship is opposite what would be required for DAT function to mediate shifts in subsecond $[DA]_o$ because faster uptake would be expected to offset $[DA]_o$ magnitude. Second, Ferris et al. (2014) directly discounted DAT as a mechanism for time-of-day shifts in $[DA]_o$ by showing that acute blockade of DAT with cocaine did not change the relationship of $[DA]_o$ magnitude across time of day. Long-term and continuous treatment with cocaine mini-pumps did, however, lead to disruptions of the diurnal rhythms in $[DA]_o$, but this is not attributed to acute mechanisms in naive rats. Rather, this disruption likely reflects the well-documented effects of long-term exposure to cocaine on DA and ACh release mechanisms, which, in turn, disrupts their time-of-day variation. Future experimentation would be necessary to understand the effects of drugs of abuse on the diurnal cycles documented here.

Moreover, our prior report also demonstrated that D2AR function was inversely related to time-of-day shift in $[DA]_o$ magnitude, with highest D2AR function at peak $[DA]_o$. Again, this relationship is opposite what would be required for D2AR rhythms to control $[DA]_o$ magnitude. Finally, extracellular DA tone is not present in brain slice preparations, suggesting that D2ARs would not have constitutive activation sufficient to mediate rhythms observed in $[DA]_o$ in a slice preparation (Phillips et al., 2002). We show that rhythms in rapid $[DA]_o$ and CIN function exist simultaneous with, and can be modified independent of, rhythms in extracellular DA tone that are mediated by changes in DAT and D2AR function. This modulation has broad implications for time-of-day variations in behaviors associated with a number of psychiatric disorders.

Working model

The overall working model for the current study is that there are times of day when an organism exhibits heightened or blunted learning and/or motivated behavior, mediated by a corresponding diurnal variation in the magnitude of DA signaling in the NAc. We show that a primary contributor of variation in DA release across time of day is differential ACh signaling from CINs in the NAc, acting directly on DA terminals via nAChRs. We show that CINs possess higher activity during the light cycle, which can increase $[DA]_o$ with stimulations that model “noise”/tonic firing, thereby decreasing the effect of the phasic DA signal and sign-tracking behavior. Conversely, relative reductions in CIN activity during the active/dark cycle increase the capacity for a greater signal-to-noise ratio of DA that is critical to drive sign-tracking behavior. For an accurate representation of how the brain mediates learning and motivation, the question is not only how the brain controls which stimuli associate and motivate action but also whether there is time-of-day variation in the associative and motivational strength of the stimuli.

Limitations of the study

Our data demonstrate diurnal rhythms in CIN modulation of DA release. However, there may be other contributing factors not explored here that could further modulate these rhythms. For example, although we are not aware of a published study, the existence of diurnal rhythms in the expression or function of nAChRs located on DA terminals in the NAc is possible. In this context, the time-of-day variation in CIN activity demonstrated here might occur in concert with variation in nAChR expression/function to manifest a higher-order rhythm for the overall influence of ACh signaling in the NAc. Another limitation of this study is that is presently unknown what mechanism is driving the time-of-day variation in CIN signaling. Such rhythms may be controlled by any one (or more) of a multitude of sources. One source could be signaling from other neurons. DA D2 receptors are located on CINs and influence their firing (Cai and Ford, 2018; Dorst et al., 2020). As noted earlier, we have already discovered diurnal variation in the function of D2 receptors in the NAc (Ferris et al., 2014). Because D2 receptors are located on CINs, it would be worth exploring whether variation in D2 function promotes rhythms in CIN firing. Additionally, the rhythmic expression of channels or proteins directly located on CINs that may be under control of circadian molecular clock genes might reveal intracellular signaling mechanisms for time-of-day shifts in CIN firing rate. The circadian molecular clock is found in all cell types in the body (Parekh et al., 2015) and functions in a transcriptional translational

feedback loop. Mutations in this molecular clock have been associated with variations in the DA system and motivated behaviors, like drug taking. For instance, *Npas2* mutant mice have variations in DA receptor expression in the NAc and decreased cocaine sensitivity (Ozburn et al., 2015). A recent report found that circadian disruptions modified the diurnal rhythms in the clock gene *Per2* and made rats more sensitive to nicotine (Balachandran et al., 2020). These data support the interplay between the cholinergic system, nAChRs, and circadian rhythms. Future experimentation, however, is needed to parse out the exact mechanisms driving the diurnal rhythms in CIN activity that affects $[DA]_o$.

STAR★METHODS

RESOURCE AVAILABILITY

Lead contact—Further information and requests for resources should be directed to and will be fulfilled by the lead contact, Mark Ferris (mferris@wakehealth.edu).

Materials availability—This study did not generate new unique materials.

Data and code availability

- All data reported in this paper will be shared by the lead contact upon request.
- This paper does not report original code.
- Any additional information required to reanalyze the data reported in this paper is available from the lead contact upon request.

EXPERIMENTAL MODEL AND SUBJECT DETAILS

Male and female wild-type Sprague-Dawley rats (375–400 g) (Harlan Laboratories, Frederick, Maryland) were used for electrical stimulation FSCV experiments and behavioral experiments. TH-cre and ChAT-cre rats bred on a Long-Evans background were used for optogenetic light-stimulation experiments and their electrical stimulation controls. Male C57BL/6 mice (~30-60 days old, Jackson Laboratory) were used for electrophysiology experiments. All animals were maintained on a 12:12 hour light/dark cycle and food and water were available *ad libitum*. Lights were either off at 4 PM and on at 4 AM for the dark cycle cohort (ZT 13 and ZT 18) or off at 7 PM and on at 7 AM for the light cycle cohort (ZT 1 and ZT 6). All experiments were performed at these exact time noted in the experiments across animals or across days by using the same lab clock for all tests. All animals were maintained according to the National Institutes of Health guidelines in Association for Assessment and Accreditation of Laboratory Animal Care (AAALAC) accredited facilities. All experimental protocols were approved by the Institutional Animal Care and Use Committee at Wake Forest School of Medicine and Brigham Young University.

METHOD DETAILS

Intracranial surgery—For optogenetic studies, TH-cre and ChAT-cre rats were anesthetized with a combination of ketamine (100 mg/kg) and xylazine (10 mg/kg), then maintained under anesthesia throughout the procedure on isoflurane (1-2%). Coordinates were located using a stereotaxic frame relative to Bregma on a leveled skull. Viral vectors

expressing channelrhodopsin (AAV-EF1a-DIO-hChR2(H134r); UNC vector core, Chapel Hill, NC) were bilaterally infused into the VTA (AP: −5.2; ML: ±0.7; DV: −7.7) or the NAc (AP: 1.5; ML: ±1.8; DV: −6.5), in TH-cre or ChAT-cre rats, respectively. Viral vectors were delivered in a volume of 100 nL/side at a rate of 0.1 uL/minute and the microsyringe was left in place for 10 minutes before withdrawal. Following surgery, rats were left in their home cages for 4-5 weeks to allow for recovery and robust viral expression.

Slice preparation—Rats were anesthetized with isoflurane and then euthanized by rapid decapitation in a ventilated area free of blood or tissue from previous animals at zeitgeber time (ZT) 1 (1 hour into light cycle), ZT 6 (6 hours into light cycle), ZT 13 (1 hour into dark cycle), or ZT 18 (6 hours into dark cycle) depending on group assignment. Rats were kept in their respective light or dark cycle at all times until brain extraction was complete. These times were chosen to encompass multiple, equally spaced times throughout both light and dark cycles. A vibrating tissue slicer (VF-300 Microtome; by Precisionary Instruments Inc., San Jose, CA) was used to prepare 400 μm thick coronal brain sections containing the NAc core, as previously described (Siciliano et al., 2017). The tissue was immersed in oxygenated, pH-adjusted (7.4) artificial cerebrospinal fluid (aCSF) containing (in mM): NaCl (126), KCl (2.5), NaH_2PO_4 (1.2), $CaCl_2$ (2.4), $MgCl_2$ (1.2), $NaHCO_3$ (25), glucose (11), and L-ascorbic acid (0.4). Brain slices were transferred to wells containing oxygenated aCSF (32°C) flowing at 1 mL/min.

Ex vivo* voltammetry—Ex vivo fast scan cyclic voltammetry* (FSCV) provides unique advantages for studying local circuit modulation of $[DA]_o$. FSCV has high spatial and temporal resolution and allows the examination $[DA]_o$ while modeling of a wide range of neuronal firing patterns (Ferris et al., 2013). Here, *ex vivo* FSCV was used to characterize diurnal rhythms in stimulated dopamine release ($[DA]_o$) in the NAc core (Fennell et al., 2020). A carbon-fiber recording microelectrode (100-200 μM length, 7 μM diameter) was placed 100-150 μM from a bipolar stimulating electrode or from a fiber optic in the NAc core. For electrical stimulation, $[DA]_o$ was evoked by a single electrical pulse (750 μA, 2 msec, monophasic) applied to the tissue every 3 minutes unless otherwise noted for a specific experiment. For light stimulation, $[DA]_o$ was evoked with light stimulation with an optical pulse (470 nM; ~21 mW, 4 ms duration) at 5 pulses and 20 Hz every 5 minutes, as done in Melchior et al. (2015). Extracellular DA was recorded by applying a triangular waveform (−0.4 to +1.2 to −0.4 V vs Ag/Agcl, 400 Vs).

Once the extracellular DA response was stable (3 consecutive collections within 10% variability), 5-pulse stimulations were applied to the slice with varying burst frequency (5, 10, 25, or 100 Hz) in order to encompass the physiological range of DA neuron firing. $[DA]_o$ following varying stimulation intensities (2 V to 7.5 V) was measured to examine intensity-response and intrinsic excitability. After assessing the DA response to varying stimulation parameters, dihydro-beta-erythroidine [DhβE; a selective β2-containing nAChR antagonist], 500 nM) was bath applied and dopamine response equilibrated to single pulse stimulation.

Electrophysiology recordings—Cell-attached recordings of CIN activity were performed in male C57 mice (~30-60 days old, Jackson Laboratory) with glass

micropipettes (2–4 MΩ) filled with aCSF. Cholinergic interneurons were identified based on their large size, tonic firing, sensitivity to muscarine, and sensitivity to Sk blockade (Yorgason et al., 2017). Data were filtered at the amplifier with a band-pass Bessel filter 0.3-3 kHz (Axon Instruments Multiclamp 700A; Molecular Devices, San Jose CA). Recordings were sampled continuously at 10 kHz with a PCIe-6321 NI-DAQ board (National Instruments, Austin, TX) and acquired using Axograph 1.7.6 (Axograph Scientific). Recordings were obtained over a 10 minute period, and the last 3 minutes of recordings were used for analysis. The firing rate was analyzed using a simple threshold detection algorithm in Axograph, and focused on measures of instantaneous firing frequency. Values reported are average instantaneous firing frequency over a 3 minute period.

***In vivo* fast scan cyclic voltammetry—**Anesthesia was induced with an intraperitoneal (IP) injection of 1.5–1.7 g/kg urethane in rats, which produced stable anesthesia throughout the duration of experiment. We then lowered a stimulating electrode into the VTA (AP: −5.2; ML: ±0.7; DV: −7.7). Dopamine release was measured in the NAc (AP: 1.5; ML: ±1.8; DV: −6.5) using a carbon fiber electrode and evoked by applying electrical stimulation parameters that mimic VTA burst firing (30p, 60Hz, monophasic+, 2 ms, 750μA) every 5 minutes. Extracellular DA was recorded by applying a triangular waveform (−0.4 to +1.2 to −0.4 V *vs* Ag/Agcl, 400 Vs).

Pavlovian conditioned approach (PCA)—Rats allowed to habituate in the animal housing facilities on their respective light:dark cycle for two weeks prior to experiments. Prior to any behavioral tasks, rats were given 1-3 sugar pellets the day before magazine training to reduce any behaviors due to the novelty of pellets. Magazine training consisted of two (minimum) or more days / sessions where animals are delivered 26 sugar pellets on a 60 second variable interval (VI) with no extended lever or cue light present (conditioned stimulus, CS). Magazine training with no CS allowed rats to learn that lever pressing is not required for sugar pellet delivery. Rats proceeded to the next phase of PCA once all pellets were consumed across two consecutive sessions. PCA sessions consisted of 27 trials where a combination lever extended and cue light turned on (CS+) for 8 seconds prior to sugar pellet delivery on a 60 second VI schedule. During PCA sessions, lever/light contacts and head entries into the food hopper were recorded to characterize sign- and goal-tracking behaviors, respectively. No operant response was required for pellet delivery in order to measure the degree to which presentation of the CS+ engendered sign-tracking behavior vs goal-tracking behavior across the light/dark cycle. After a minimum of five sessions, and when behaviors did not vary by 25% across 2 session, rats then received an injection of subcutaneous nicotine (0.4 mg/kg) or saline 15 minutes prior to a final PCA session. Videos were also taken to ensure that rats were awake and behaving.

Drugs—Dihydro-β-erythroidine hydrobromide ((2*S*,13b*S*)-2-Methoxy-2,3,5,6,8,9,10,13-octahydro-1*H*,12*H*-benzo[*i*]pyrano[3,4-*g*]indolizin-12-one hydrobromide; Tocris Bioscience, Bristol, UK) was dissolved in distilled water. 1 mM concentration aliquots were stored at −20°C or 4°C and diluted with oxygenated aCSF to final concentration before bath

application on slices. (−)-Nicotine hydrogen tartrate was purchased from Sigma (St. Louis, MO), dissolved in sterile saline, and pH adjusted prior to subcutaneous injection.

QUANTIFICATION AND STATISTICAL ANALYSIS

Data acquisition and modeling—Demon Voltammetry and Analysis software was used to acquire and model FSCV data (Yorgason et al., 2011). Recording electrodes were calibrated by recording electrical current responses (in nA) to a known concentration of dopamine (3 mM) using a flow-injection system. This was used to convert electrical current to dopamine concentration (Ferris et al., 2013).

Statistical analysis—Baseline $[DA]_o$ to single-pulse stimulations (raw numbers and percent change) were compared by students t-test. Baseline $[DA]_o$ to multi-pulse stimulations and paired-pulse ratio were compared by two-way mixed-factor ANOVA. Baseline $[DA]_o$ following drug application (including percent change, normalized to 1 pulse pre-drug baseline, and paired-pulse ratio) were compared by three-factor generalized linear mixed model analysis. In the case of significant interactions, Bonferroni or Tukey post-hoc comparisons were used. Graph Pad Prism (version 8, La Jolla, CA) were used to statistically analyze data sets ($\alpha = 0.05$) and compose graphs. Data are presented as mean ± SEM for group data across multiple variables or mean with individual data points for bar graphs.

Supplementary Material

Refer to Web version on PubMed Central for supplementary material.

ACKNOWLEDGMENTS

We would like to acknowledge Lacey Sexton for technical contributions. This work was supported by National Institutes of Health grants R01 DA052460 (to M.J.F.), R00 DA031791 (to M.J.F.), P50 DA006634 (to M.J.F. and K.F.R.-G.), P50 AA025117 (to M.J.F. and K.F.R.-G.), R01 NS105005 (to K.F.R.-G.), R01 AA026551 (to K.F.R.-G.), F32 AA028162 (to E.G.P.), and F31 DA053114 (to A.C.L.); Alzheimer's Association grants AARF-19-614794 (to F.N.) and AARG-NTF-21-852843 (to K.F.R.-G.); Department of Defense grant USAMRMC W81XWH-14-1-0061 (to K.F.R.-G.); and the Peter McManus Charitable Trust (to M.J.F.).

REFERENCES

Acosta J, Bussi IL, Esquivel M, Höcht C, Golombek DA, and Agostino PV (2020). Circadian modulation of motivation in mice. Behav. Brain Res 382, 112471. 10.1016/j.bbr.2020.112471. [PubMed: 31958519]

Adamantidis AR, Zhang F, Aravanis AM, Deisseroth K, and de Lecea L (2007). Neural substrates of awakening probed with optogenetic control of hypocretin neurons. Nature 450, 420–424. 10.1038/nature06310. [PubMed: 17943086]

Balachandran RC, Hatcher KM, Sieg ML, Sullivan EK, Molina LM, Mahoney MM, and Eubig PA (2020). Pharmacological challenges examining the underlying mechanism of altered response inhibition and attention duetocircadian disruption in adult Long-Evans rats. Pharmacol. Biochem. Behav 193, 172915. 10.1016/j.pbb.2020.172915. [PubMed: 32224058]

Beckmann JS, Marusich JA, Gipson CD, and Bardo MT (2011). Novelty seeking, incentive salience and acquisition of cocaine self-administration in the rat. Behav. Brain Res 216, 159–165. 10.1016/j.bbr.2010.07.022. [PubMed: 20655954]

Bennett BD, and Wilson CJ (1999). Spontaneous activity of neostriatal cholinergic interneurons in vitro. J. Neurosci 19, 5586–5596. 10.1523/JNEUROSCI.19-13-05586.1999. [PubMed: 10377365]

Berke J (2018). What does dopamine mean? Nat. Neurosci 21, 787–793. 10.1038/s41593-018-0152-y. [PubMed: 29760524]

Brimblecombe KR, Threlfell S, Dautan D, Kosillo P, Mena-Segovia J, and Cragg SJ (2018). Targeted activation of cholinergic interneurons accounts for the modulation of dopamine by striatal nicotinic receptors. ENeuro 5, ENEURO.0397-17.2018. 10.1523/ENEURO.0397-17.2018.

Cachope R, Mateo Y, Mathur BN, Irving J, Wang H-L, Morales M, Lovinger DM, and Cheer JF (2012). Selective activation of cholinergic interneurons enhances accumbal phasic dopamine release: setting the tone for reward processing. Cell Rep. 2, 33–41. 10.1016/j.celrep.2012.05.011. [PubMed: 22840394]

Cai Y, and Ford FP (2018). Dopamine cells differentially regulate striatal cholinergic transmission across regions through corelease of dopamine and glutamate. Cell Rep. 25, 3148–3157. 10.1016/j.celrep.2018.11.053. [PubMed: 30540946]

Castañeda TR, Prado B. M. de, Prieto D, and Mora F (2004). Circadian rhythms of dopamine, glutamate and GABA in the striatum and nucleus accumbens of the awake rat: modulation by light. J. Pineal Res 36, 177–185. 10.1046/j.1600-079X.2003.00114.x. [PubMed: 15009508]

Cheer JF, Wassum KM, Heien MLAV, Phillips PEM, and Wightman RM (2004). Cannabinoids enhance subsecond dopamine release in the nucleus accumbens of awake rats. J. Neurosci 24, 4393–4400. 10.1523/JNEUROSCI.0529-04.2004. [PubMed: 15128853]

Clark JJ, Collins AL, Sanford CA, and Phillips PEM (2013). Dopamine encoding of Pavlovian incentive stimuli diminishes with extended training. J. Neurosci. Off. J. Soc. Neurosci 33, 3526–3532. 10.1523/JNEUROSCI.5119-12.2013.

Condon MD, Platt NJ, Zhang Y-F, Roberts BM, Clements MA, Vietti-Michelina S, Tseu M-Y, Brimblecombe KR, Threlfell S, Mann EO, and Cragg SJ (2019). Plasticity in striatal dopamine release is governed by release-independent depression and the dopamine transporter. Nat. Commun 10, 4263. 10.1038/s41467-019-12264-9. [PubMed: 31537790]

Cragg SJ (2003). Variable dopamine release probability and short-term plasticity between functional domains of the primate striatum. J. Neurosci 23, 4378–4385. 10.1523/JNEUROSCI.23-10-04378.2003. [PubMed: 12764127]

DePoy LM, McClung CA, and Logan RW (2017). Neural mechanisms of circadian regulation of natural and drug reward. Neural Plast. 2017, 5720842. 10.1155/2017/5720842. [PubMed: 29359051]

Dibner C, Schibler U, and Albrecht U (2010). The mammalian circadian timing system: organization and coordination of central and peripheral clocks. Annu. Rev. Physiol 72, 517–549. 10.1146/annurev-physiol-021909-135821. [PubMed: 20148687]

Dorst MC, Tokarska A, Zhou M, Lee K, Stagkourakis S, Broberger C, Masmanidis S, and Silberber G (2020). Polysynaptic inhibition between striatal cholinergic interneurons shapes their network activity patterns in a dopmaine-dependent manner. Nat. Commun 11, 5113. [PubMed: 33037215]

Ferris MJ, Calipari ES, Yorgason JT, and Jones SR (2013). Examining the complex regulation and drug-induced plasticity of dopamine release and uptake using voltammetry in brain slices. ACS Chem. Neurosci 4, 693–703. 10.1021/cn400026v. [PubMed: 23581570]

Ferris MJ, España RA, Locke JL, Konstantopoulos JK, Rose JH, Chen R, and Jones SR (2014). Dopamine transporters govern diurnal variation in extracellular dopamine tone. Proc. Natl. Acad. Sci 111, E2751–E2759. 10.1073/pnas.1407935111. [PubMed: 24979798]

Flagel SB, Watson SJ, Robinson TE, and Akil H (2007). Individual differences in the propensity to approach signals vs goals promote different adaptations in the dopamine system of rats. Psychopharmacology 191, 599–607. 10.1007/s00213-006-0535-8. [PubMed: 16972103]

Flagel SB, Clark JJ, Robinson TE, Mayo L, Czuj A, Willuhn I, Akers CA, Clinton SM, Phillips PEM, and Akil H (2011). A selective role for dopamine in stimulus–reward learning. Nature 469, 53–57. 10.1038/nature09588. [PubMed: 21150898]

Grace A, and Bunney B (1984). The control of firing pattern in nigral dopamine neurons: single spike firing. J. Neurosci 4, 2866–2876. 10.1523/JNEUROSCI.04-11-02866.1984. [PubMed: 6150070]

John CE, and Jones SR (2006). Exocytotic release of dopamine in ventral tegmental area slices from C57BL/6 and dopamine transporter knockout mice. Neurochem. Int 49, 737–745. 10.1016/j.neuint.2006.06.004. [PubMed: 16901588]

McClung CA (2007). Circadian rhythms, the mesolimbic dopaminergic circuit, and drug addiction. ScientificWorldJournal 7, 194–202. 10.1100/tsw.2007.213. [PubMed: 17982593]

Melchior JR, Ferris MJ, Stuber GD, Riddle DR, and Jones SR (2015). Optogenetic versus electrical stimulation of dopamine terminals in the nucleus accumbens reveals local modulation of presynaptic release. J. Neurochem 134, 833–844. 10.1111/jnc.13177. [PubMed: 26011081]

Negus SS, Mello NK, Portoghese PS, Lukas SE, and Mendelson JH (1995). Role of delta opioid receptors in the reinforcing and discriminative stimulus effects of cocaine in rhesus monkeys. J. Pharmacol. Exp. Ther 273, 1245–1256. [PubMed: 7791097]

Nolan SO, Zachry JE, Johnson AR, Brady LI, Siciliano CA, and Calipari ES (2020). Direct dopamine terminal regulation by local striatal microcircuitry. J. Neurochem 155, 475–493. 10.1111/jnc.15034. [PubMed: 32356315]

Ozburn AR, Falcon E, Twaddle A, Nugent AL, Gillman AG, Spencer SM, Arey RN, Mukherjee S, Lyons-Weiler J, Self DW, and McClung CA (2015). Direct regulation of diurnal Drd3 expression and cocaine reward by NPAS2. Biol. Psychiatr. 77, 425–33. 10.1016/j.biopsych.2014.07.030.

Palmatier MI, Marks KR, Jones SA, Freeman KS, Wissman KM, and Sheppard AB (2013). The effect of nicotine on sign-tracking and goal-tracking in a Pavlovian conditioned approach paradigm in rats. Psychopharmacology 226, 247–259. 10.1007/s00213-012-2892-9. [PubMed: 23090624]

Parekh PK, Ozburn AR, and McClung CA (2015). Circadian clock genes: effects on dopamine, reward and addiction. Alcohol (Fayetteville, N.Y.) 49, 341–349. 10.1016/j.alcohol.2014.09.034.

Paulson PE, and Robinson TE (1994). Relationship between circadian changes in spontaneous motor activity and dorsal versus ventral striatal dopamine neurotransmission assessed with on-line microdialysis. Behav. Neurosci 108, 624–635. 10.1037//0735-7044.108.3.624. [PubMed: 7917055]

Phillips PEM, Hancock PJ, and Stamford JA (2002). Time window of autoreceptor-mediated inhibition of limbic and striatal dopamine release. Synapse (New York, N.Y.) 44, 15–22. 10.1002/syn.10049.

Pidoplichko VI, DeBiasi M, Williams JT, and Dani JA (1997). Nicotine activates and desensitizes midbrain dopamine neurons. Nature 390, 401–404. 10.1038/37120. [PubMed: 9389479]

Ren Z-Y, Zhang X-L, Liu Y, Zhao L-Y, Shi J, Bao Y, Zhang XY, Kosten TR, and Lu L (2009). Diurnal variation in cue-induced responses among protracted abstinent heroin users. Pharmacol. Biochem. Behav 91, 468–472. 10.1016/j.pbb.2008.08.023. [PubMed: 18809427]

Rice ME, and Cragg SJ (2004). Nicotine amplifies reward-related dopamine signals in striatum. Nat. Neurosci 7, 583–584. 10.1038/nn1244. [PubMed: 15146188]

Roberts DCS, Brebner K, Vincler M, and Lynch WJ (2002). Patterns of cocaine self-administration in rats produced by various access conditions under a discrete trials procedure. Drug Alcohol Depend. 67, 291–299. 10.1016/S0376-8716(02)00083-2. [PubMed: 12127200]

Robinson DL, Heien MLAV, and Wightman RM (2002). Frequency of dopamine concentration transients increases in dorsal and ventral striatum of male rats during introduction of conspecifics. J. Neurosci 22, 10477–10486. 10.1523/JNEUROSCI.22-23-10477.2002. [PubMed: 12451147]

Saunders BT, and Robinson TE (2013). Individual variation in resisting temptation: implications for addiction. Neurosci. Biobehav. Rev 37, 1955–1975. 10.1016/j.neubiorev.2013.02.008. [PubMed: 23438893]

Saunders BT, O'Donnell EG, Aurbach EL, and Robinson TE (2014). A cocaine context renews drug seeking preferentially in a subset of individuals. Neuropsychopharmacology 39, 2816–2823. 10.1038/npp.2014.131. [PubMed: 24896613]

Sharpe MJ, Chang CY, Liu MA, Batchelor HM, Mueller LE, Jones JL, Niv Y, and Schoenbaum G (2017). Dopamine transients are sufficient and necessary for acquisition of model-based associations. Nat. Neurosci 20, 735–742. 10.1038/nn.4538. [PubMed: 28368385]

Siciliano CA, McIntosh JM, Jones SR, and Ferris MJ (2017). α6β2 sub-unit containing nicotinic acetylcholine receptors exert opposing actions on rapid dopamine signaling in the nucleus accumbens of rats with high-versus low-response to novelty. Neuropharmacology 126, 281–291. 10.1016/j.neuropharm.2017.06.028. [PubMed: 28666811]

Steinberg EE, Keiflin R, Boivin JR, Witten IB, Deisseroth K, and Janak PH (2013). A causal link between prediction errors, dopamine neurons and learning. Nat. Neurosci 16, 966–973. 10.1038/nn.3413. [PubMed: 23708143]

Terman M, and Terman JS (1970). Circadian rhythm of brain self-stimulation behavior. Science 168, 1242–1244. 10.1126/science.168.3936.1242. [PubMed: 5442714]

Terman M, and Terman JS (1975). Control of the rat's circadian self-stimulation rhythm by light-dark cycles. Physiol. Behav 14, 781–789. 10.1016/0031-9384(75)90070-0. [PubMed: 1187832]

Threlfell S, Lalic T, Platt NJ, Jennings KA, Deisseroth K, and Cragg SJ (2012). Striatal dopamine release is triggered by synchronized activity in cholinergic interneurons. Neuron 75, 58–64. 10.1016/j.neuron.2012.04.038. [PubMed: 22794260]

Webb IC (2017). Circadian rhythms and substance abuse: chronobiological considerations for the treatment of addiction. Curr. Psychiatr. Rep 19, 12. 10.1007/s11920-017-0764-z.

Whitton AE, Mehta M, Ironside ML, Murray G, and Pizzagalli DA (2018). Evidence of a diurnal rhythm in implicit reward learning. Chronobiol. Int 35, 1104–1114. 10.1080/07420528.2018.1459662. [PubMed: 29688082]

Yorgason JT, España RA, and Jones SR (2011). Demon voltammetry and analysis software: analysis of cocaine-induced alterations in dopamine signaling using multiple kinetic measures. J. Neurosci. Methods 202, 158–164. 10.1016/j.jneumeth.2011.03.001. [PubMed: 21392532]

Yorgason JT, Zeppenfeld DM, and Williams JT (2017). Cholinergic interneurons underlie spontaneous dopamine release in nucleus accumbens. J. Neurosci 37, 2086–2096. 10.1523/JNEUROSCI.3064-16.2017. [PubMed: 28115487]

Zhang H, and Sulzer D (2004). Frequency-dependent modulation of dopamine release by nicotine. Nat. Neurosci 7, 581–582. 10.1038/nn1243. [PubMed: 15146187]

Zhang T, Zhang L, Liang Y, Siapas AG, Zhou F-M, and Dani JA (2009). Dopamine signaling differences in the nucleus accumbens and dorsal striatum exploited by nicotine. J. Neurosci 29, 4035–4043. 10.1523/JNEUROSCI.0261-09.2009. [PubMed: 19339599]

Zhou FM, Liang Y, and Dani JA (2001). Endogenous nicotinic cholinergic activity regulates dopamine release in the striatum. Nat. Neurosci 4, 1224–1229. 10.1038/nn769. [PubMed: 11713470]

Highlights

- Dopamine release magnitude exhibits diurnal rhythms
- Cholinergic interneuron activity exhibits diurnal rhythms
- There is diurnal variation in cholinergic interneuron modulation of dopamine release
- Cue-directed conditioned responses are exclusive to rats in their dark cycle

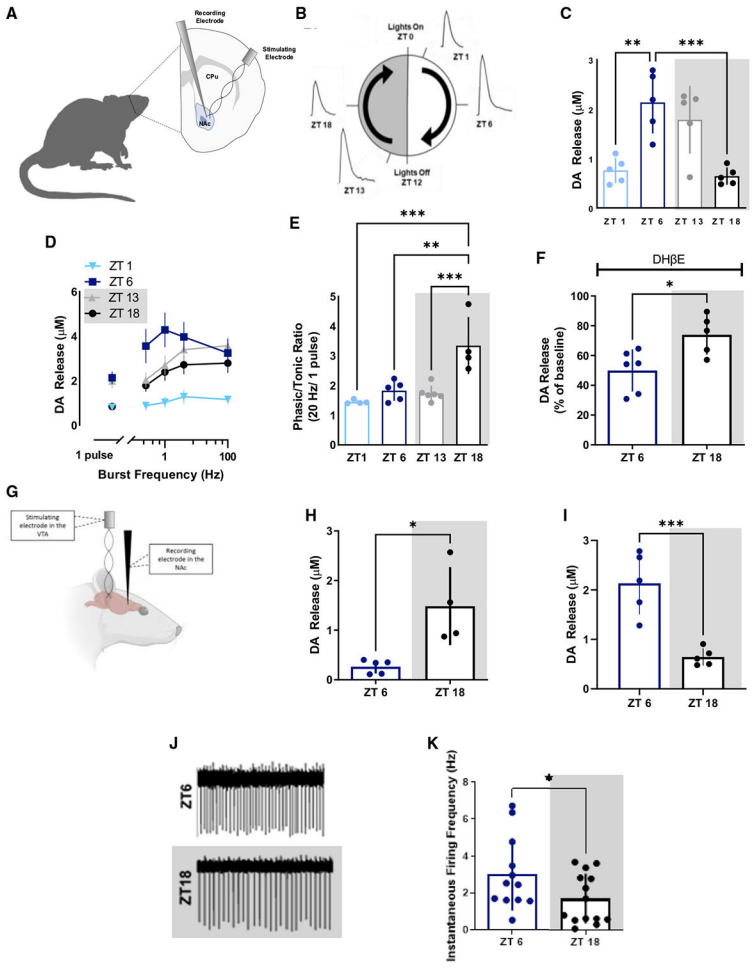

Figure 1. FSCV and electrophysiology determine diurnal variations in DA and cholinergic signaling in the in the NAc core

(A) Schematic of *ex vivo* FSCV used to examine dopamine (DA) release in the *nucleus accumbens* (NAc) core in male and female rats.

(B) All rats were sacrificed at zeitgeber time (ZT) 1 (1 h into the light cycle), ZT 6 (6 h into the light cycle), ZT 13 (1 h into the dark cycle), or ZT 18 (6 h into the dark cycle). Representative traces of $[DA]_o$ after single-pulse electrical stimulation is presented for each time point.

(C) $[DA]_o$ after single-pulse stimulation was measured at different time points to assess time-of-day variation in stimulated $[DA]_o$ magnitude and was higher at ZT 6 relative to ZT 1 and ZT 18 (n = 4–5 per group).

(D) $[DA]_o$ was elicited using 5 electrical pulses at increasing frequencies to model *in vivo* tonic and phasic firing. $[DA]_o$ is higher at ZT 6 across low but not higher frequencies in comparison with ZT 18 (n = 5 per group).

(E) Phasic/tonic ratios (20 Hz/1 pulse stimulation) were higher at ZT 18 than all other time-points (n = 4–5 per group).

(F) $[DA]_o$ expressed as a percentage of baseline was examined after bath application of DHβE. DHβE reduced DA release significantly more at ZT6 in comparison with ZT 18 (n = 5–6 per group).

(G) Schematic of *in vivo* voltammetry with electrical stimulation in the ventral tegmental area (VTA) and recording in the NAc core.
(H and I) Higher $[DA]_o$ in the NAc core at ZT 18 in comparison with ZT 6 using *in vivo* voltammetry to simulated cell bodies in the VTA (H), which is opposite of what is observed using *ex vivo* voltammetry $[DA]_o$ (I; n = 4–5 per group).
(J) Instantaneous NAc cholinergic (CIN) firing, as measured by cell-attached single-unit recordings.
(K) NAc CIN firing was, on average, ~76% higher at ZT 6 compared with ZT 18 time points.
Bars represent means ± SEM, and dots indicate individual data points. Shaded regions behind data represent the dark cycle (lights off). *p < 0.05, **p < 0.01, ***p < 0.001.

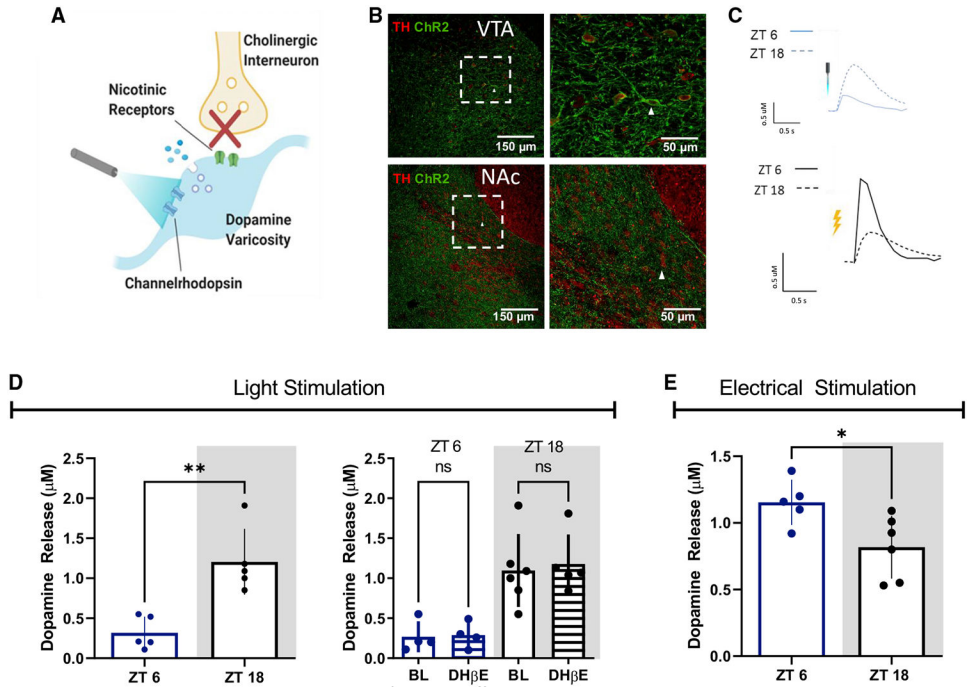

Figure 2. Selective stimulation of DA release midway during the light (ZT 6) and dark (ZT 18) cycle using optogenetics

(A) We injected ChR2-eYFP into the VTA of TH-cre rats. 4–5 weeks later, we used *ex vivo* voltammetry paired with blue light stimulation (470 nM, 21.8 mW) to selectively target DA terminals in the NAc without the effect of CINs.

(B) Expression of ChR2-eYFP in the VTA (top left panel) and higher magnification of expression in the VTA (top right panel) and expression of ChR2-eYFP in the NAc (bottom left panel) and at higher magnitude (bottom right panel). In all panels, midbrain DA neurons were immunolabeled for tyrosine hydroxlyase (TH; red), with a merged overlay showing ChR2-eYFP (green).

(C and D) Left panels: light stimulation of $[DA]_o$ is significantly higher at ZT 18 than at ZT 6 (n = 5). Right panels: to confirm that the $[DA]_o$ was from DA neurons alone, we used DHβE to block any potential contribution from ACh. DHβE did not modulate $[DA]_o$ at either time point.

(E) Electrical stimulation of $[DA]_o$ in the same tissue/location, in contrast, is greater at ZT 6 (n = 4–6), as before.

Bars represent means ± SEM, and dots indicate individual data points. Shaded regions behind data represent the dark cycle (lights off). *p < 0.05, **p < 0.01.

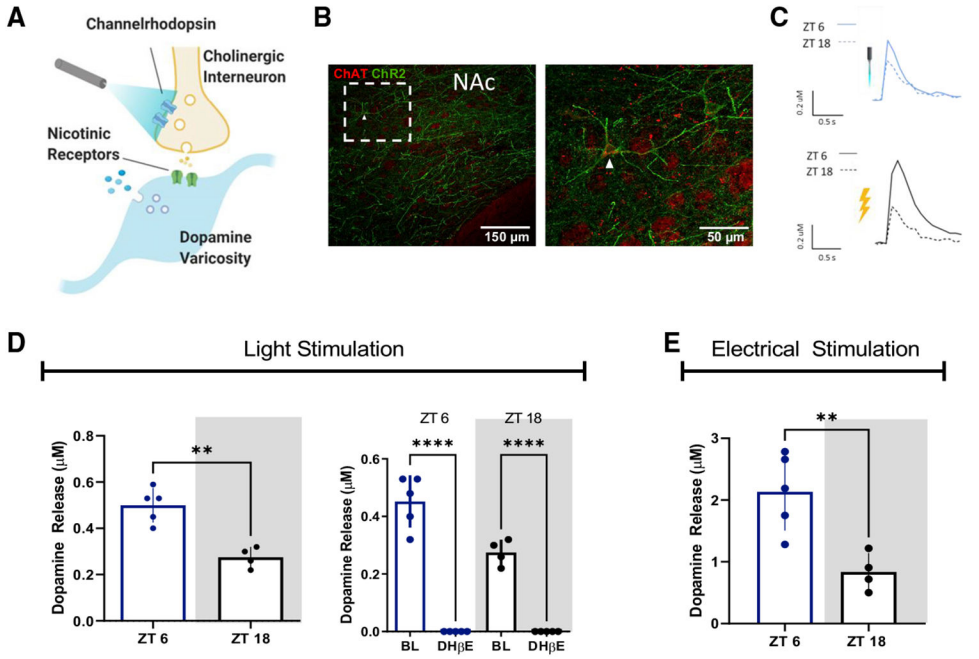

Figure 3. Selective stimulation of CINs midway during the light (ZT 6) and dark (ZT 18) cycle using optogenetics

(A) We injected channelrhodopsin2 (ChR2)-eYFP into the NAc of ChAT-cre rats and then used blue light stimulation (470 nM, 21.8 mW) of cholinergic interneurons (CINs) in the NAc after 4–5 weeks to examine time-of-day variation in ACh control over DA release. (B) Expression of ChR2-eYFP in the nucleus NAc (left panel) and higher-magnification image (right panel) showing expression on the CINs. In both panels, cells containing choline acteyltransferase (ChAT) are immunolabeled (red), with a merged overlay showing ChR2-eYFP expression (green). (C and D) CIN-driven $[DA]_o$ is greater at ZT 6 than at ZT 18 (n = 5) (D, left panel). We applied DHβE as a control to ensure that light-stimulated $[DA]_o$ was driven by ACh modulation. DHβE completely eliminates light-stimulated $[DA]_o$, indicating that we are measuring ACh-driven $[DA]_o$ (n = 5) (D, right panel). (E) Electrical stimulation of $[DA]_o$ in the same tissue/location is also greater at ZT 6 (n = 4–6), as before (n = 5). Bars represent means ± SEM, and dots indicate individual data points. Shaded regions behind data represent the dark cycle (lights off). *p < 0.05, **p < 0.01, ****p < 0.0001.

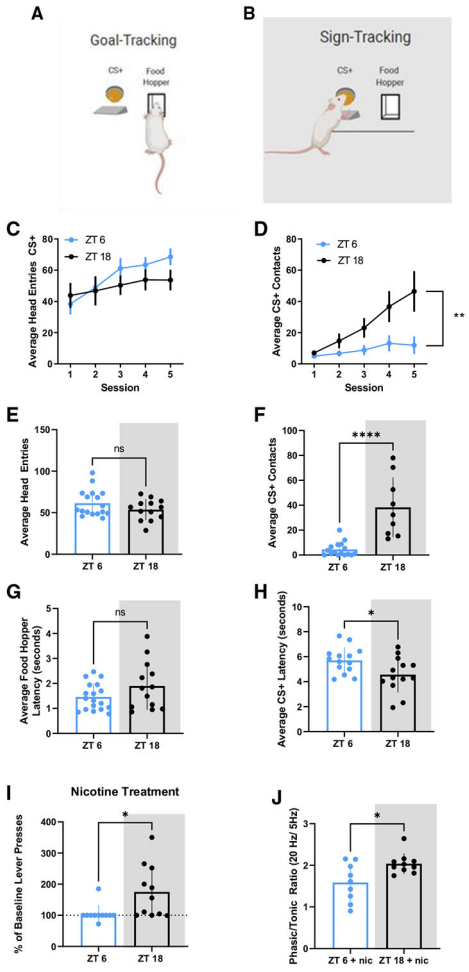

Figure 4. Diurnal rhythms in conditioned responses to reward cues with and without nicotine administration

(A) Schematic of goal-tracking behaviors during the Pavlovian conditioned approach (PCA), observed during ZT 6 and ZT 18.

(B) Schematic of sign-tracking behaviors during the PCA, which are exclusively observed in rats at ZT 18 (shaded for lights off).

(C) Learning curves for goal-tracking behaviors that show average head entries into the food hopper during the conditioned stimulus presentation (CS+) across sessions (n = 12–18).

(D) Learning curves for sign-tracking behaviors (CS+ contacts) during the CS+ ON across sessions.

(E) There are no significant differences in head entries into the food hopper during the CS+ (goal tracking) between rats at ZT 6 and ZT 18, which supports that rats were awake and engaging with the task at both time points. Data are expressed as the average head entries during the last 3 sessions.

(F) Higher CS+ contacts (sign tracking) in rats at ZT 18 in comparison with ZT 6, expressed as average of the last 3 sessions.

(G) No significant differences in latency to first head entry into the food hopper during CS+ between rats at ZT 6 and ZT 18.

(H) Lower latency to first CS+ contact in rats at ZT 18 in comparison with rats at ZT 6.

(I) Nicotine pre-treatment exclusively enhanced CS+ contacts in rats at ZT 18 (n = 12).
(J) After PCA, nicotine enhanced phasic/tonic ratios at ZT 18 in comparison with ZT 6 using *ex vivo* FSCV (n = 9–11).
Bars represent means ± SEM, and dots indicate individual data points. Shaded regions behind data represent the dark cycle (lights off). *p < 0.05, **p < 0.01.

KEY RESOURCES TABLE

REAGENT or RESOURCE	SOURCE	IDENTIFIER
Antibodies		
Tyrosine Hydroxylase Rabbit polyclonal	Fisher Scientific , Invitrogen manufacturer	Cat#P21962; RRID: AB_1088125
Donkey anti-Rabbit Alexa Fluor 594	abcam	Cat# ab150076; RRID: AB_2782993
Anti-Green Fluorescent Protein Chicken Polyclonal	abcam	Cat# ab13970
Goat anti-Chicken Alexa Fluor 488	Fisher Scientific, Invitrogen manufacturer	Cat# A11039; RRID: AB_2534096
Choline Acetyltransferase Goat Polyclonal	Fisher Scientific, MilliporeSigma Manufacturer	Cat# AB144PMI; RRID: AB_2079594
Anti-Green Fluorescent Protein Rabbit Polyclonal	abcam	Cat# ab65
Donkey anti-Goat Alexa Fluor 594	Fisher Scientific, Invitrogen Manufacturer	Cat# A11058; RRID: AB_2534105
Donkey anti-Rabbit Alexa Fluor 488	Fisher Scientific, Invitrogen Manufacturer	Cat# A21206; RRID: AB_2556546
Bacterial and virus strains		
AAV5-EF1a-DIO-hChR2(H134R)-EYFP-WPRE-PA	The Vector Core at University of North Carolina at Chapel Hill (UNC Vector Core)	N/A
Chemicals, peptides, and recombinant proteins		
Urethane	Sigma-Aldrich	Cat#U2500
(−)-Nicotine Hydrogen Tartrate salt. Minimum 98%	Sigma-Aldrich	N5260
Dihydro-β-Erythroidine Hydrobromide	Tocris Bioscience	Cat#2349 PubChem 11957537
Experimental models: Organisms/strains		
Rattus: Sprague Dawley	Envigo	Hsd:Sprague Dawley SD
Rattus: Strain: LE-Tg(TH-Cre)3.1 Deis Long Evans background with mutation type of transgenic mouse Tyrosine Hydroxylase gene Cre Recombinase (mouse Th promoter)	Rat Resource and Research Center	RRID:RRRC_00659 RRRC #659 LE-Tg(TH-Cre)3.1Deis
Rattus: Strain: LE-Tg(Chat-Cre)5.1 Deis Long Evans background with mutation type of transgenic mouse choline acetyltransferase gene Cre Recombinase (mouse Chat promoter)	Rat Resource and Research Center	RRID:RRRC_00658 RRRC#658 LE-Tg(Chat-CRE)5.1 Deis
Mus: Strain #:00064 C57BL/6 mice	The Jackson Laboratory	RRID:IMSR_JAX:000664
Software and algorithms		
Demon Voltammetry and Analysis	Wake Forest University School of Medicine	N/A
Med Associates Med-PC IV	Med Associates	SOF-735
Axograph Version 1.7.6	AxoGraph	https://axograph.com